Journal of Astronomical Telescopes, Instruments, and Systems

AstronomicalTelescopes.SPIEDigitalLibrary.org

# Daylight operation of a sodium laser guide star for adaptive optics wavefront sensing

Michael Hart
Stuart M. Jefferies
Neil Murphy

SPIE.

Michael Hart, Stuart M. Jefferies, Neil Murphy, "Daylight operation of a sodium laser guide star for adaptive optics wavefront sensing," *J. Astron. Telesc. Instrum. Syst.* **2**(4), 040501 (2016), doi: 10.1117/1.JATIS.2.4.040501.

# Daylight operation of a sodium laser guide star for adaptive optics wavefront sensing

**Michael Hart,[a,b,*] Stuart M. Jefferies,[b,c] and Neil Murphy[d]**
[a]University of Arizona, College of Optical Sciences, 1630 East University Boulevard, Tucson, Arizona 85721, United States
[b]University of Hawai'i, Institute for Astronomy, 34 Ohia Ku Street, Pukalani, Hawaii 96768, United States
[c]Georgia State University, Department of Physics and Astronomy, 25 Park Place, Atlanta, Georgia 30303, United States
[d]Jet Propulsion Laboratory, Mail Stop 180 600, 4800 Oak Grove Drive, Pasadena, California 91109, United States

**Abstract.** We report contrast measurements of a sodium resonance guide star against the daylight sky when observed through a tuned magneto-optical filter (MOF). The guide star was created by projection of a laser beam at 589.16 nm into the mesospheric sodium layer and the observations were made with a collocated 1.5-m telescope. While MOFs are used with sodium light detecting and ranging systems during the day to improve the signal-to-noise ratio of the measurements, they have not so far been employed with laser guide stars to drive adaptive optics (AO) systems to correct atmospherically induced image blur. We interpret our results in terms of the performance of AO systems for astronomy, with particular emphasis on thermal infrared observations at the next generation of extremely large telescopes now being built.
 [DOI: 10.1117/1.JATIS.2.4.040501]

Keywords: adaptive optics; laser guide star; daylight observing; wavefront sensing.

Paper 16031L received Jun. 22, 2016; accepted for publication Oct. 13, 2016; published online Oct. 26, 2016.

## 1 Introduction and Motivation

Laser guide stars (LGSs) are an effective means to extend the sky coverage and scientific value of adaptive optics (AO) systems operating at astronomical telescopes. Indeed, most large observatories around the world now employ beacons generated by resonant backscatter of laser light at the $D_2$ line of 589.16 nm from atomic sodium in the mesosphere. Beckers and Cacciani[1] suggested that the value of extremely large telescopes (ELTs) in the 25-m class and larger could be extended by using them to make high-resolution observations in thermal infrared (IR) wavelengths during the day since the limitation imposed by the bright sky background in these bands is no worse than at night. They noted that such telescopes would benefit from laser-guided AO correction at wavelengths of 3.5 $\mu$m and longer, though telescopes of the time were already diffraction limited in that regime. While there are, of course, serious practical challenges to operating a large telescope when the sun is above the horizon, there is also a significant advantage. The scientific return on the substantial investment in ELTs that is now being made could be substantially extended by taking advantage of daylight hours not required for maintenance tasks. The three major ELT projects—the European Extremely Large Telescope (EELT),[2] the Giant Magellan Telescope (GMT),[3] and the Thirty Meter Telescope (TMT)[4]—are all planning AO systems driven by signals from multiple sodium LGS and could, in principle, benefit from the approach. What is needed is a tool to allow the LGS to be used effectively when seen against the bright sky background at the beacon wavelength. Beckers and Cacciani noted that this could be done by placing the wavefront sensor (WFS) behind a sodium atomic vapor filter. Such filters are referred to in the literature as Faraday anomalous dispersion optical filters or magneto-optical filters (MOF). Here, we adopt the MOF naming convention. The MOF has a number of desirable characteristics including high throughput, wavelength stability, and wide angular acceptance. Most importantly, it offers a bandpass of <10 pm, which is sufficiently narrow to block almost all the scattered sunlight but wide enough to admit all the LGS light.[5]

Sodium laser systems designed to probe atmospheric properties through light detecting and ranging have employed MOFs to permit daylight operation.[6,7] These systems have different requirements from LGS for AO, typically using lasers with low pulse rates at tens of hertz,[8,9] and great care is needed to stabilize the center frequency of the laser and the temperature of the MOF to obtain accurate windspeed measurements.[7,10,11] In contrast, LGS must operate at frame rates of ~1000 Hz and stability is required only at a level that maintains an adequate return flux. To our knowledge, no measurements have been made of the achievable contrast from the resonant backscatter during the day with a view to establishing the viability of its use as an LGS. We report such measurements in this paper and explore the implications for AO wavefront sensing on an ELT.

## 2 Description of the Experiment

The University of Arizona (UA) has a sodium laser on long-term loan from the US Air Force Research Laboratory. The laser generates ~6.5 W of narrowband continuous-wave light in a beam that is circularly polarized to take advantage of optical pumping.[12] It is installed on an optical bench next to the UA's 1.5-m Kuiper telescope on Mount Bigelow in Arizona. The beam has a Gaussian profile and is launched through a 10-cm aperture that is separated from the Kuiper telescope's optical axis by ~5 m. For the experiment described in this paper, the laser launch projector was pointed at zenith and the Kuiper telescope pointed slightly off zenith to place the sodium resonance beacon at about a 90-km range within its field of view. A simple instrument bolted to the Cassegrain focus of the Kuiper telescope included an imaging camera behind a sodium MOF from the Eddy Company (Apple Valley, California). We used this arrangement to evaluate the potential for using a sodium LGS for daytime wavefront sensing.

The basic MOF consists of a cell that contains an atomic vapor placed between crossed linear polarizers in a kilogauss-level magnetic field. The magnetic field results in both Zeeman splitting of the atomic resonance lines in the vapor and a

*Address all correspondence to: Michael Hart, E-mail: mhart@optics.arizona.edu

2329-4124/2016/$25.00 © 2016 SPIE

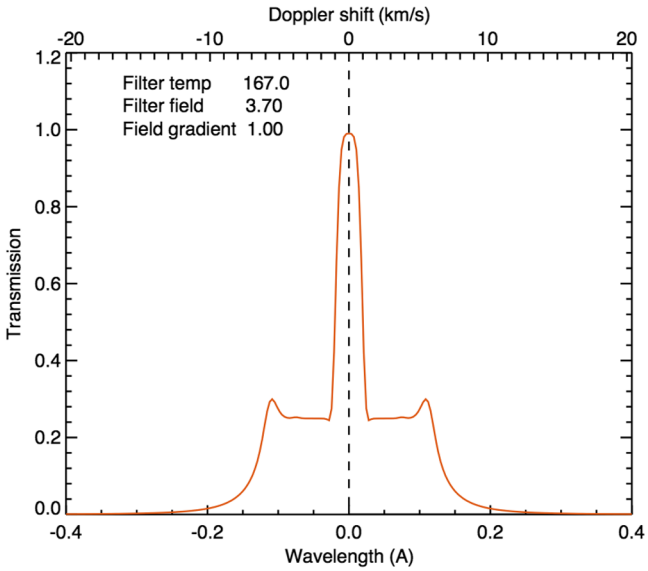


**Fig. 1** Theoretical transmission curve for linearly polarized light at the entrance window of an MOF with a longitudinal magnetic field strength of 3.7 kG, operating at a temperature of 167°C.

variation of the polarization-dependent absorption coefficient and refractive index (anomalous dispersion) with wavelength across the vapor absorption lines. A suitable choice of vapor temperature and magnetic field strength results in the absorption and birefringence profiles producing wavelength-dependent transmission in the vicinity of the resonance lines through rotation of the polarization.[13] At the wavelength of peak transmission, a linearly polarized beam with axis aligned to the first polarizer will be rotated in the vapor cell to align precisely with the axis of the second polarizer. Under these conditions, the theoretical transmission maximum for the MOF configuration used in the work reported here (longitudinal magnetic field strength 3.7 kG, temperature $167 \pm 0.1$°C) is close to 100% (Fig. 1), without accounting for transmission losses in the optics. To maximize the LGS signal at our detector, we placed a high-transmission ($T = 0.995$) zero-order quarter-wave plate (QWP) in front of the MOF to convert the circularly polarized return laser light into linearly polarized light with the axis aligned to the first polarizer of the MOF.

Practically, a narrowband interference filter is required in front of the MOF to suppress off-band leakage through the polarizers. Figure 2 shows the measured transmission of the optics of our MOF with the vapor cell cold and polarizers uncrossed: the width of the profile in this condition is determined

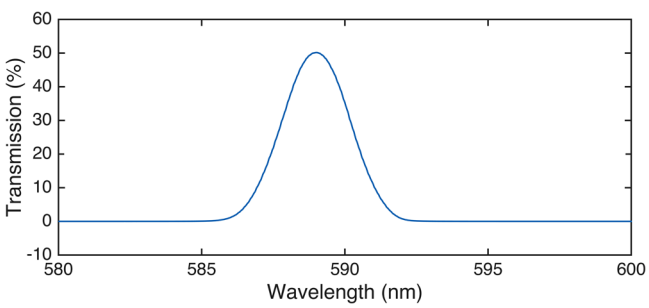


**Fig. 2** Transmission curve of the cold MOF with uncrossed polarizers. The profile is determined by the interference filter ahead of the MOF itself.

by the interference filter. The peak at 0.5 is commensurate with the manufacturers' transmission values for the components: 0.82 for the polarizers, 0.75 for the narrowband interference filter, and 0.995 for each of the windows of the sodium vapor cell. We note that polarizers and interference filters with higher transmission values are available which would increase the transmission of the MOF optics to 0.76. For detection, we use a Point Grey Flea3 camera in 12-bit mode. To allow us to compute absolute photometry of the LGS, we determined the mean gain of the camera by measuring a photon transfer curve.[14] The result of 2.96 e − /ADU is in good agreement with the manufacturer's specification of 3.0 e − /ADU.

After acquiring the LGS on the imaging camera, we focused the 1.5-m telescope at the height of the mesospheric sodium layer. Continuous sequences of 200 to 500 images were recorded at 4 frames/s with individual exposure times of 0.25 s. Figure 3

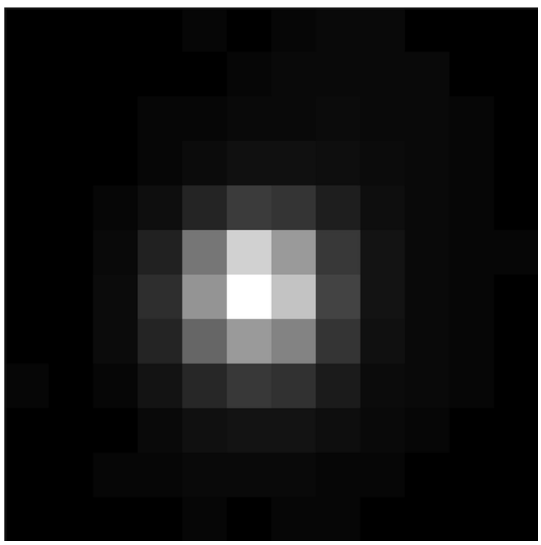

**Fig. 3** The LGS seen against the daytime sky at 07:04 local time. The exposure time is 8 s and the pixel scale is 2.5 arc sec.

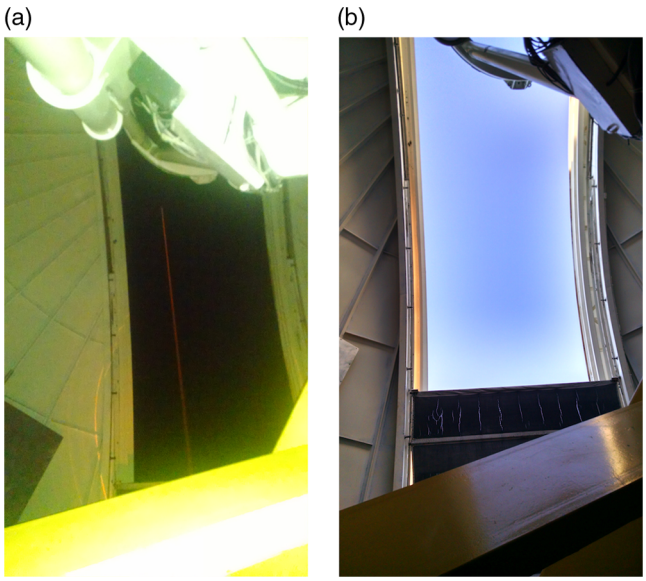


**Fig. 4** (a) The laser beam propagating to zenith through the slit of the Kuiper telescope dome is easily seen at night. (b) Approximately the same view in daylight when the beam is very hard to see.

shows the LGS seen through the MOF in an integration of 8 s, the sum of 32 exposures, recorded during daylight, ~42 min after sunrise. The LGS has a full width at half maximum of 3.1 arc sec, which is the result of a combination of seeing and diffraction of the Gaussian beam profile at the launch aperture. The image scale on our camera was 0.156 arc sec /pixel, which for analysis was binned by 16× to 2.5 arc sec /pixel.

We observed the characteristics of the LGS from 00:00 local time (07:00 UTC) to 07:04 local time (14:04 UTC) on March 24, 2016. As local sunrise was at 06:22 (13:22 UTC), this provided observations during both nighttime and daytime conditions. The change in contrast between the laser light and the background sky is nicely shown in the photographs in Fig. 4.

## 3 Results

The MOF transmission was estimated from nighttime sequences of LGS images with and without the MOF installed in the optical beam from the telescope. Maximum transmission was ensured by careful alignment of the QWP and polarizer axes and by adjusting the MOF operating temperature. The measured fluxes with and without the MOF were, respectively, $8.4 \times 10^5$ and $1.90 \times 10^6$ photons $m^{-2}$ $s^{-1}$, implying a transmission for the whole MOF of 0.44. This value is consistent with expectations when two additional sources of reduced transmission are included. First, a scan of the wavelength of the laser revealed that the central passband of our MOF was shifted 0.001 nm from the wavelength of the sodium atoms in the mesosphere by the buffer gas used in the vapor cell. This reduced the transmission by an additional factor of 0.92. Second, the temperature of our narrowband interference filter was not stabilized and the difference between the ambient temperature in the telescope dome and the design operating temperature for the filter resulted in a 0.35-nm shift in the center passband, leading to a transmission reduction of 0.97.

Table 1 shows the LGS and sky brightness as seen through the MOF as the sun rose. The LGS brightness was found to remain approximately constant over the time frame of these observations at a mean value of $1.20 \times 10^6$ photons $m^{-2}$ $s^{-1}$. This is consistent with previous measurements[15] given our output power at the time of ~6.5 W, the low Na column density of $2.5 \times 10^9$ $cm^{-2}$ expected in early spring, about half the annual mean,[16] and the overall transmission of the system which we

**Table 1** LGS and sky brightness results.

| Sequence start time | Sky brightness (photon $m^{-2}$ $s^{-1}$ arc $sec^{-2}$) | LGS brightness (photon $m^{-2}$ $s^{-1}$) |
|---|---|---|
| 06:33:33 | 961 | $1.27 \times 10^6$ |
| 06:50:38 | 957 | $1.18 \times 10^6$ |
| 06:52:49 | 1050 | $1.14 \times 10^6$ |
| 06:54:58 | 1060 | $1.22 \times 10^6$ |
| 06:57:07 | 1090 | $1.26 \times 10^6$ |
| 06:59:17 | 1070 | $1.12 \times 10^6$ |
| 07:01:36 | 1040 | $1.19 \times 10^6$ |
| 07:03:50 | 1080 | $1.18 \times 10^6$ |

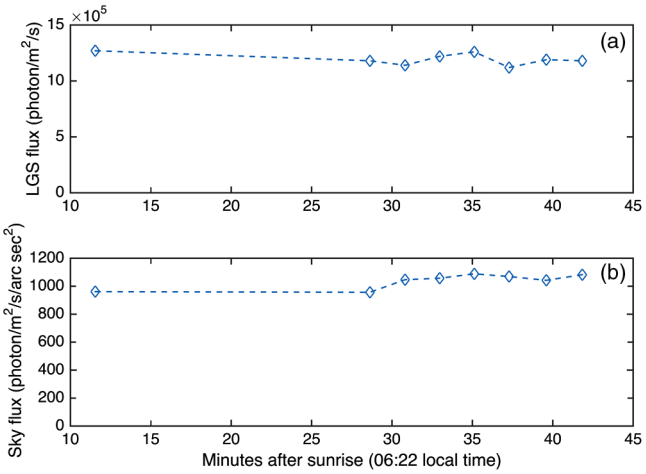


**Fig. 5** (a) Flux from the LGS in the period after sunrise. (b) Simultaneous measurements of the background flux from the sky.

estimate to be 0.19. The telescope itself, with two bare aluminum-coated mirrors, has a throughput of ≈0.8; the relay optics comprising two protected silver fold mirrors, an AR-coated collimating lens and the QWP, contribute a factor of 0.95; the measured transmission of the MOF is 0.44; and the Flea3 quantum efficiency at 589 nm is quoted by the manufacturer to be 0.56. This would imply a flux at the telescope aperture of $1.0 \times 10^6$ photons $m^{-2}$ $s^{-1}$ $W^{-1}$, although we note that the uncertainty in this estimate is unquantified.

The results of Table 1 are shown graphically in Fig. 5. The sky background, immeasurably low by our camera during the night, remains low throughout the period of the observations at about 1000 to 1100 photons $m^2$ $s^{-1}$ arc $sec^{-2}$ until the end of the sequence, about 45 min after sunrise when the sun was ~80 deg from the beacon at zenith. Unfortunately, observations had to cease at that time to avoid subjecting the telescope head ring to direct sunlight.

## 4 Wavefront Sensing for Extremely Large Telescopes

From these quantitative measurements of LGS flux and sky background through the MOF, we can calculate the expected signal-to-noise ratio (SNR) for a WFS operating during the day on an ELT. We expect some loss of signal because of the imperfect transmission of the filter and the photon noise from background illumination will certainly be higher than at night. We note, however, that most astronomical AO systems are designed to correct wave fronts in bands down to the near-IR, at 2 $\mu$m or shorter, including the laser-guided systems for the three ELTs, while daylight observing at those telescopes is likely to be restricted to bands at 3.5 $\mu$m and longer. In this regime, the AO system requirements on speed and spatial sampling of the wave front are reduced, so lost SNR may, if necessary, be recovered by longer integrations or larger subapertures on the WFS.

As a case study, we consider the LGS WFS of the TMT's Narrow Field InfraRed AO System (NFIRAOS).[17,18] These are six of the Shack–Hartmann type, with square subapertures 0.5 m on a side, running nominally at 800 frames/s. Each WFS sees the return from a single sodium LGS generated by a laser of ~20 W. Although the lasers are launched from behind the telescope's secondary mirror, parallax causes the image of the LGS to be elongated by as much as 4 arc sec as seen by subapertures

at the outer edge of the pupil. The field of view of these subapertures is, therefore, rather large at $3 \times 7.5$ arc sec, comprising 90 pixels of 0.5 arc sec dimension. Assuming, rather pessimistically, an overall photon efficiency not significantly different than we saw at the Kuiper telescope, the laser flux during the day would be 1150 photons/subaperture/frame and the mean sky flux through the MOF would be just 8.2 photons/subaperture/frame. This is comparable to the unfiltered flux that would be seen from a sky of visual magnitude 18 arc sec$^{-2}$, conditions typical of a dark site at night under a full moon. The uncertainty in the WFS signal would be dominated by the shot noise from the LGS, the desirable regime in which to operate. The SNR per subaperture is given by $L/(L + S + n^2P)^{1/2}$, where $L$ and $S$ are, respectively, the observed LGS and sky fluxes, $P$ is the pixel count in the subaperture, and $n$ is the rms read noise/pixel. Assuming $n = 3\,\mathrm{e}^-$, the SNR would be about 25. Provided that $S < n^2P$, the SNR will not be significantly reduced by the sky background. In our experiments, conducted at solar elongations between 80 deg and 90 deg, this inequality is satisfied by two orders of magnitude. Given such a wide margin, sodium LGS would be usable to within a few degrees of the solar disk. As a matter of practicality, however, it is likely that the ELTs will require much larger solar exclusion angles in order to prevent direct illumination of the telescope optics by the sun.

At 3.5 $\mu$m, the shortest wavelength where daytime operation at the ELTs might be considered, characteristic nighttime values of the Fried parameter $r_0$ will be about 1.5 m. However, a number of site test studies for solar telescopes show that, after a period of relatively good seeing shortly after sunrise, the seeing may worsen by a factor of 2 to 3 as convection develops.[19–21] We would then expect $r_0 \approx 0.5$ m. With worse seeing, several effects conspire to degrade AO system performance, notably an increase in fitting error by the deformable mirrors and reduced WFS sensitivity because of the enlarged LGS spot size. The increased background noise in the WFS will have negligible impact thanks to the MOF, and we do not expect a significant change in tomographic projection errors in the analysis of the six WFS signals because almost all the degradation in seeing arises in the ground layer. The fitting error scales approximately as $r_0^{-5/6}$. Working from details provided by Gilles et al.[18] on the wavefront error budget of NFIRAOS, we predict this term will rise from 63 to 157 nm rms. The effect of spot size is harder to evaluate without a full system model, but conservatively, neglecting detector effects, the noise in the wavefront gradients deteriorates linearly with reduced $r_0$. At worst then, the 41 nm rms WFS noise term would degrade to 123 nm. The entire TMT wavefront error budget would then increase from 187 nm rms[17] to about 260 nm rms. This is still adequate to support diffraction-limited imaging at 3.5 $\mu$m with 80% Strehl ratio.

AO requires image motion correction that cannot be provided by the LGS measurements. In addition, the mean height of the sodium layer varies on time scales of minutes which leads to focus errors in the wavefront correction if the effect is not accounted for. As with nighttime operation, these modes must be sensed with a natural guide star. This will need to be in the IR, both to lower the sky noise and to take advantage of the image sharpening afforded by the AO, which improves the star's SNR when seen against a diffuse background. Beckers[22] notes that there are enough stars in the J to K bands to offer full coverage in the Galactic plane, although coverage is only partial at the poles. We believe, then, that our results demonstrate the feasibility of daytime AO operation at the ELTs for observations in the thermal IR.

## Acknowledgments

We thank C. Denman and P. Hillman of FASORtronics LLC for their support in operating the laser. We are most grateful to the Mountain Operations team of Steward Observatory for technical assistance with the telescope and to R.P. Scott for acting as the telescope operator. S.M.J. acknowledges support from the US Air Force Office of Scientific Research through Contract FA9550-14-1-0178.

## References

1. J. M. Beckers and A. Cacciani, "Using laser beacons for daytime adaptive optics," *Exp. Astron.* **11**, 133–143 (2001).
2. E. Diolaiti et al., "Conceptual design and performance of the multiconjugate adaptive optics module for the European extremely large telescope," *Proc. SPIE* **7736**, 77360R (2010).
3. A. H. Bouchez et al., "The Giant Magellan telescope adaptive optics program," *Proc. SPIE* **9148**, 91480W (2014).
4. C. Boyer et al., "Adaptive optics program at TMT," *Proc. SPIE* **9148**, 91480X (2014).
5. A. Cacciani and A. M. Fofi, "The magneto-optical filter II: velocity field measurements," *Sol. Phys.* **59**, 179–189 (1978).
6. H. Chen et al., "Daytime operation of Na temperature lidar using a dispersive Faraday vapor filter," *Proc. SPIE* **2833**, 46–52 (1996).
7. C. Y. She et al., "The first 80-hour continuous LIDAR campaign for simultaneous observation of mesopause region temperature and wind," *Geophys. Res. Lett.* **30** (2003).
8. T. Pfrommer, P. Hickson, and C. Y. She, "A large-aperture sodium fluorescence LIDAR with very high resolution for mesopause dynamics and adaptive optics studies," *Geophys. Res. Lett.* **36** (2009).
9. X. Hu et al., "Sodium fluorescence doppler LIDAR to measure atmospherecr temperature in the mesopause region," *Chin. Sci. Bull.* **56**, 417–423 (2011).
10. C. Y. She et al., "High-spectral-resolution fluorescence light detection and ranging for mesospheric sodium temperature measurements," *Appl. Opt.* **31**, 2095–2106 (1992).
11. Y. Yang et al., "A flat spectral Faraday filter for sodium LIDAR," *Opt. Lett.* **36**, 1302–1304 (2011).
12. J. C. Bienfang et al., "20 W of continuous-wave sodium D2 resonance radiation from sum-frequency generation with injection-locked lasers," *Opt. Lett.* **28**, 2219–2221 (2003).
13. W. Kiefer et al., "Na-Faraday rotation filtering: the optimal point," *Nat. Sci. Rep.* **4**, 1–7 (2014).
14. J. R. Janesick, K. P. Klaasen, and T. Elliott, "Charge-coupled-device charge-collection efficiency and the photon-transfer technique," *Opt. Eng.* **26**, 972–980 (1987).
15. J. Ge et al., "Simultaneous measurements of sodium column density and laser guide star brightness," *Proc. SPIE* **3353**, 242–253 (1998).
16. G. C. Papen, C. S. Gardner, and G. Yu, "Characterization of the mesospheric sodium layer," in *OSA Conf. on Adaptive Optics, OSA Technical Digest Series*, Vol. 13, pp. 96–99, OSA, Washington, DC (1996).
17. B. Ellerbroek et al., "The TMT adaptive optics program," in *Second Int. Conf. on Adaptive Optics for Extremely Large Telescopes* (2011).
18. L. Gilles, L. Wang, and B. Ellerbroek, "Modeling update for the thirty meter telescope laser guide star dual-conjugate adaptive optics system," *Proc. SPIE* **7736**, 77360W (2010).
19. F. C. M. Bettonvil et al., "The enclosure for the European solar telescope (EST)," *Proc. SPIE* **7733**, 773333 (2010).
20. G. B. Scharmer and T. I. M. van Werkhoven, "S-DIMM+ height characterization of day-time seeing using solar granulation," *Astron. Astrophys.* **513**, A25 (2010).
21. T. Rimmele, "Haleakala turbulence and wind profiles used for adaptive optics performance modeling," ATST Project Document RPT-0030, Advanced Technology Solar Telescope, Tucson, Arizona (2006).
22. J. M. Beckers, "Daytime observations with extremely large telescopes in the thermal infrared using laser guide star adaptive optics," in *Adaptive Optics for Extremely Large Telescopes II* (2011).